State-to-state dynamics of the $Cl+CH_3OH \rightarrow HCl+CH_2OH$ reaction

Hans A. Bechtel, Jon P. Camden, and Richard N. Zare[a)]
Department of Chemistry, Stanford University, Stanford, California 94305-5080

(Received 20 November 2003; accepted 8 December 2003)

Molecular chlorine, methanol, and helium are co-expanded into a vacuum chamber using a custom designed ''late-mixing'' nozzle. The title reaction is initiated by photolysis of Cl_2 at 355 nm, which generates monoenergetic Cl atoms that react with CH_3OH at a collision energy of 1960 ± 170 cm^{-1} (0.24 ± 0.02 eV). Rovibrational state distributions of the nascent HCl products are obtained via $2+1$ resonance enhanced multiphoton ionization, center-of-mass scattering distributions are measured by the core-extraction technique, and the average internal energy of the CH_3OH co-products is deduced by measuring the spatial anisotropy of the HCl products. The majority ($84\pm7\%$) of the HCl reaction products are formed in HCl($v=0$) with an average rotational energy of $\langle E_{rot}\rangle = 390\pm70$ cm^{-1}. The remaining $16\pm7\%$ are formed in HCl($v=1$) and have an average rotational energy of $\langle E_{rot}\rangle = 190\pm30$ cm^{-1}. The HCl($v=1$) products are primarily forward scattered, and they are formed in coincidence with CH_2OH products that have little internal energy. In contrast, the HCl($v=0$) products are formed in coincidence with CH_2OH products that have significant internal energy. These results indicate that two or more different mechanisms are responsible for the dynamics in the $Cl+CH_3OH$ reaction. We suggest that (1) the HCl($v=1$) products are formed primarily from collisions at high impact parameter via a stripping mechanism in which the CH_2OH co-products act as spectators, and (2) the HCl($v=0$) products are formed from collisions over a wide range of impact parameters, resulting in both a stripping mechanism and a rebound mechanism in which the CH_2OH co-products are active participants. In all cases, the reaction of fast Cl atoms with CH_3OH is with the hydrogen atoms on the methyl group, not the hydrogen on the hydroxyl group. © *2004 American Institute of Physics.* [DOI: 10.1063/1.1644797]

I. INTRODUCTION

The field of reaction dynamics aims to gain a microscopic understanding of chemical transformations by investigating reactions at an unprecedented level of detail. The approach often taken is the so-called ''asymptotic'' approach: by preparing the reagents in well-defined quantum states and meticulously measuring the final product states, insight is gained into the molecular forces that influence the interaction of the reagents in the transition state region. Because of their reduced dimensionality, atom-plus-diatom reactions have typically been the most straightforward systems to study. Extensive experimental measurements and sophisticated theoretical treatments have led to a nearly complete picture of the dynamics of many prototypical reactions, including the simplest chemical reaction of all: the $H+H_2$ bimolecular exchange reaction. In contrast, less information is known about reactions involving polyatomic reagents because the increased degrees of freedom generally complicate experimental and theoretical investigations. Polyatomic reactions, however, have their own set of questions that are intriguing for chemists because they address fundamental concepts that are applicable only to systems of greater chemical complexity. Is the reaction localized at a particular site? Can the reaction be accelerated by exciting one type of nuclear motion rather than another? If the reagent has multiple reaction sites, how do they compete? How is excess energy disposed among the newly formed bonds and the old, nonreacting bonds? Are the nonreacting bonds spectators or active participants in the reaction?

Although numerous experiments have attempted to address these and other questions in reactions of F,[1–10] Cl,[11–19] and O[20–33] with saturated hydrocarbons, relatively few measurements have focused on the dynamics and the product energy disposal in hydrogen abstraction reactions involving oxygenated polyatomic organic molecules, such as alcohols.[34–41] The reactions of methanol are particularly interesting because methanol is the simplest organic molecule having two distinct reaction sites, arising from the abstraction of hydrogen from either the methyl group to form the hydroxymethyl radical CH_2OH or from the hydroxyl group to form the methoxy radical CH_3O. For the $Cl+CH_3OH$ reaction, the former channel is exothermic (at 0 K) $\Delta H_0 = -2780\pm120$ cm^{-1} (-0.34 ± 0.01 eV),[42,43] whereas the latter channel is slightly endothermic $\Delta H_0 = 250\pm350$ cm^{-1} (0.03 ± 0.04 eV).[43,44] Kinetic measurements have shown that the total rate constant is $(5.4\pm0.9)\times10^{-11}$ cm^3 $molecule^{-1}$ s^{-1} at 295 ± 2 K,[45] with the CH_2OH channel occurring ~95% of the time.[46]

Ahmed *et al.*[38,39] previously obtained the angular distributions of the hydroxyalkyl products from the reactions of Cl with methanol, ethanol, and isopropanol by combining crossed molecular beam techniques with velocity map imaging. Although photolysis backgrounds created large uncertainties in the extreme forward-scattered region, they con-

a)Author to whom correspondence should be addressed. Electronic mail: zare@stanford.edu

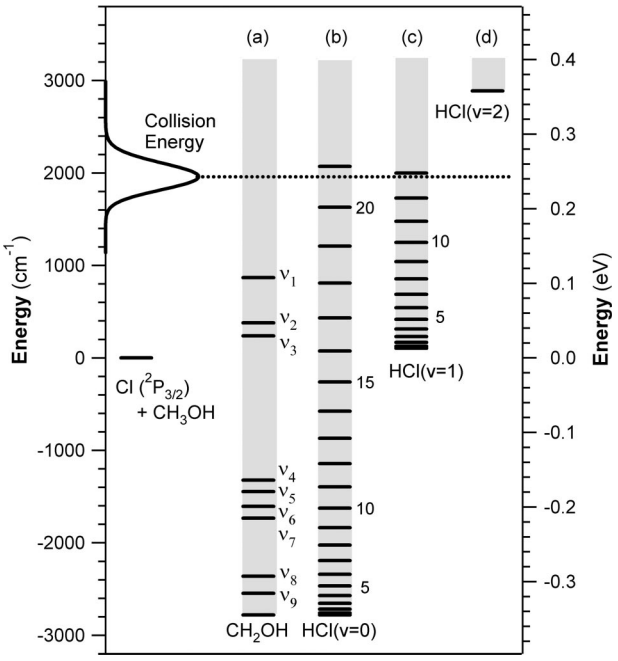

FIG. 1. Energy level diagram for the reaction of atomic chlorine with methanol to form HCl and CH_2OH. Photolysis of Cl_2 at 355 nm provides 1960 cm^{-1} (0.24 eV) of collision energy with an energy spread determined from the formulas of van der Zande *et al.* (Ref. 52) using a translational temperature of 10 K. Channel (a) shows the fundamental vibrational modes of the CH_2OH radical product. Channels (b) and (c) show the rotational states of the HCl($v=0$) and HCl($v=1$) products. Channel (d) represents the HCl($v=2$) products, which are energetically not allowed. Although the CH_3O+HCl channel is energetically allowed, it is not observed in the present experiments.

cluded that the hydroxyalkyl products are predominantly scattered in the backward-sideways direction with respect to the alcohol beam direction, suggesting direct rebound dynamics. These conclusions indicate that the shallow well present in the $Cl+CH_3OH$ *ab initio* potential energy surface[47,48] is not deep enough to cause long-lived intermediate complexes. Recently, Rudić *et al.*[40,41] measured the rotational distribution of the HCl($v=0$) products from the reaction of Cl atoms with methanol, ethanol, and dimethyl ether. In all cases, they observed a larger degree of rotational excitation from these reactions than from reactions of atomic Cl with alkanes. They attributed this result to dipole–dipole interactions in the exit channel of the potential energy surface.

Here, we examine the dynamics and energy disposal of the $Cl+CH_3OH$ reaction by investigating the state distributions of the HCl products, the state-selected scattering distributions of the HCl($v=1$) products, and the correlated average internal energy present in the CH_2OH products. Figure 1 displays the energetics of the CH_2OH channel along with the product states allowed at the collision energy employed in this experiment (1960 ± 170 cm^{-1}). After providing a brief experimental overview, we present the rotational distributions of the HCl($v=0$) and HCl($v=1$) products. Then, we discuss how spatial anisotropy measurements provide a means of determining the average internal energy present in the unobserved CH_2OH product, which allows us to convert the measured product speed distributions into state-resolved angular distributions. Finally, we compare the dynamics and energy disposal of this reaction with other reactions, including the $Cl+CH_4(v_3=1)$ and $Cl+C_2H_6$ reactions, and present several mechanisms that may account for the observed dynamics.

II. EXPERIMENT

The *photoloc* method and experimental apparatus have been described previously;[12,49] therefore, only the primary features are presented here. The reagents, molecular chlorine (Matheson, 99.999%, 10% in He) and methanol (neat or 25% in He), are stored in separate glass bulbs. Each reagent is connected to a pulsed valve (General Valve, Series 9) that regulates the gas flow into a custom faceplate to allow mixing of the two reagents before they supersonically co-expand into a vacuum chamber through a single 0.8 mm orifice. This ''late-mixing nozzle,'' described in detail elsewhere,[50] was designed to eliminate buildup of HCl products from the prereaction of Cl_2 with CH_3OH, while maintaining supersonic conditions necessary for translational cooling. The methanol backing pressure was maintained at 120 or 250 Torr, and the Cl_2 backing pressure was increased to maintain a total pressure of 3×10^{-5} Torr in the reaction chamber. Velocity measurements of the HCl contaminant in the Cl_2 mixture indicate that the translational temperature is less than 10 K.[50]

The reaction is initiated by the photolysis of Cl_2 with linearly polarized 355 nm light from the third harmonic of a Nd^{3+}:YAG laser (Continuum PL9020). At this wavelength, more than 99% of the Cl atoms are produced in the ground state ($^2P_{3/2}$) with an angular anisotropy parameter of $\beta_{Cl}=-0.98\pm0.05$.[51] The photolysis wavelength determines the relative motion between the reagents and forms a near-Gaussian distribution[52] of center-of-mass collision energies, centered at 1960 cm^{-1} (0.24 eV) with a HWHM of 170 cm^{-1} (0.02 eV), assuming a translational temperature of 10 K. The photolysis laser ($\sim$50 mJ/pulse) is loosely focused by an $f=45$ cm lens. Under these experimental conditions, measurements of β_{Cl} were in good agreement with literature values.

The HCl products are allowed to accumulate for 60–200 ns before they are state selectively ionized by 2+1 resonance-enhanced multiphoton ionization (REMPI), separated by mass in a Wiley–McLaren time-of-flight (TOF) mass spectrometer, and detected by microchannel plates. At 0 ns delay no reaction signal is observed, and the signal grows linearly with time, indicating that the observed products do not arise from chlorine–methanol clusters. The probe light for the HCl REMPI is generated by doubling the output of a dye laser (Lambda Physik FL2002 using Exciton LD489), which is pumped by a Nd^{3+}:YAG laser (Quanta Ray DCR-2A). The dye laser beam is focused using an $f=50$ cm lens, and typical probe laser energies are 2.5 mJ/pulse. The HCl products are detected via the $F\,^1\Delta_2-X\,^1\Sigma(0,0)$, the $f\,^3\Delta_2-X\,^1\Sigma(0,0)$, the $F\,^1\Delta_2-X\,^1\Sigma(1,1)$, and the $E\,^1\Sigma-X\,^1\Sigma(0,1)$ bands.[53–60] Intensities of spectral lines are converted into relative populations by using correction factors obtained by recording spectra of HCl at room temperature. Our measured correction factors are in good agreement with previously published correction factors.[12,14,40,41,61] HCl backgrounds resulting from

impurities in the Cl_2 are small relative to the reaction signal; however, their contribution to the signal is removed by operating the photolysis light at half the repetition rate of the probe laser.

The product velocity distributions are measured using Wiley–McLaren[62] space-focusing conditions in combination with a core-extractor that masks products with velocity components perpendicular to the TOF detection axis. The measured lab-frame velocity of the reaction product $\vec{v}_{\mathrm{prod}}$ is the vector sum of the center-of-mass velocity $\vec{u}_{\mathrm{com}}$, determined by the photolysis of Cl_2, and the reaction product center-of-mass frame velocity $\vec{u}_{\mathrm{HCl}}$, determined by the energetics of the reaction, the state-selection of the HCl product, and the internal energy of the CH_2OH co-product.[63] The determination of these two vectors and measurement of the product speed distribution uniquely determines three sides of a triangle. Using the law of cosines, the measured lab-frame velocity distribution can be transformed into a distribution of scattering angles in the center-of-mass frame. The transformation of the laboratory speed distribution to a differential cross section (DCS) is based on knowledge of the internal energy of the co-product. For atom/diatom reactions, detection of the diatomic product uniquely constrains the energy of the atomic product. In reactions with polyatomic reagents, however, the undetected products may have significant amounts of internal energy in the extra rotational and vibrational degrees of freedom. Thus, an additional measurement of the angle between the center-of-mass velocity and the lab-frame product velocity, $\boldsymbol{\alpha}$, is required to determine $\vec{u}_{\mathrm{HCl}}$. Although $\boldsymbol{\alpha}$ cannot be measured directly in the current experiment, measuring the spatial anisotropy of the reaction product $\beta(v)$ gives an averaged value related to $\boldsymbol{\alpha}$ that provides additional information about the internal energy of the undetected product. This measurement is carried out by changing the direction of the photolysis laser beam polarization between parallel and perpendicular to the TOF axis on an every-other-shot basis using a photo-elastic modulator (PEM-80, Hinds International Inc.). This procedure provides the isotropic $\mathbf{I}_{\mathrm{iso}}=\mathbf{I}_{\parallel}+2\mathbf{I}_{\perp}$ and anisotropic $\mathbf{I}_{\mathrm{aniso}}=2(\mathbf{I}_{\parallel}-\mathbf{I}_{\perp})$ components of the TOF profiles, which are analyzed by a method described in detail by Simpson *et al.*[49]

III. RESULTS

A. Rotational state distributions

Figure 2 shows the rotational distributions of the HCl($v=0$, J) and HCl($v=1$, J) products from the $Cl+CH_3OH$ reaction. The HCl($v=0$) REMPI spectra are obtained by scanning the probe laser over members of the *Q*, *R*, and *S* branches of the $F\,^1\Delta_2-X\,^1\Sigma(0,0)$ band and the *Q*-branch of the $f\,^3\Delta_2-X\,^1\Sigma(0,0)$ band, whereas the HCl($v=1$) products are detected via the *R* and *S* branches of the $F\,^1\Delta_2-X\,^1\Sigma(1,1)$ band and the *Q*-branch of the $E\,^1\Sigma-X\,^1\Sigma(0,1)$ band. All errors represent 95% confidence intervals of replicate measurements. The HCl($v=0$) products have an average rotational energy of $\langle E_{\mathrm{rot}}\rangle=390\pm70\,\mathrm{cm}^{-1}$, and the HCl($v=1$) products have an average rotational energy of $\langle E_{\mathrm{rot}}\rangle=190\pm30\,\mathrm{cm}^{-1}$. The HCl($v=0$) rotational distributions are in excellent agreement with the previous measurements of Rudic *et al.*[40,41] By comparing the relative intensities of the $R(1)$ and $R(5)$ lines of the $F\,^1\Delta_2-X\,^1\Sigma(1,1)$ and the $F\,^1\Delta_2-X\,^1\Sigma(0,0)$ bands, respectively, and applying the appropriate correction factors,[12] we are able to obtain the branching ratio of the HCl($v=1$) to HCl($v=0$) products: 0.19 ± 0.09. Thus, $16\pm7\%$ of the reaction products are formed in HCl($v=1$), and the remaining $84\pm7\%$ are formed in HCl($v=0$). Rotationally relaxed kinetic measurements[64] have previously indicated that the fraction of vibrationally excited HCl was $12\pm2\%$, which agrees well with our measurements of the nascent HCl products.

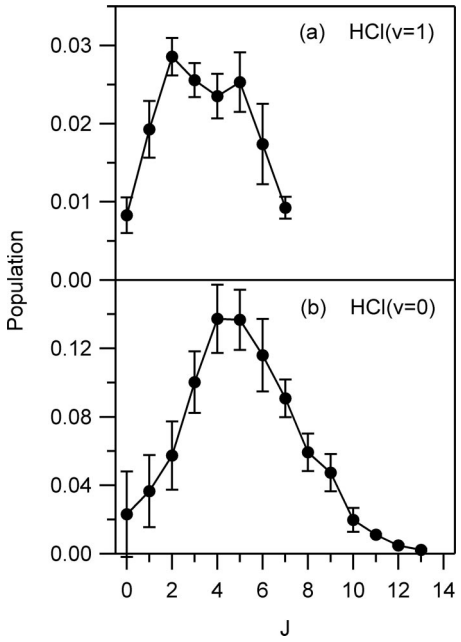

FIG. 2. Rotational distributions of the (a) HCl($v=1$, J) and (b) HCl($v=0$, J) products from the reaction of atomic chlorine with methanol. The HCl($v=0$, J) and HCl($v=1$, J) populations are scaled such that the sum over all products is equal to 1 [$\Sigma\, P(v,\, J)=1$], and the error bars represent 95% confidence intervals of replicate measurements.

As discussed above, HCl product formation can come from two channels to form either hydroxymethyl radical (CH_2OH) or methoxy radical (CH_3O). To examine the different channels we used two different isotopomers, CH_3OD and CD_3OH. For the $Cl+CH_3OD$ reaction, we did not observe any DCl products within our signal-to-noise ratio, and the observed HCl rotational distribution was nearly identical to that of the $Cl+CH_3OH$ reaction. Similarly, for the $Cl+CD_3OH$ reaction, we only observed DCl products. Thus, we conclude that our measured HCl rotational distributions from the $Cl+CH_3OH$ reaction come entirely from hydrogen abstraction from one of the three hydrogens on the methyl group.

B. HCl($v=1$) speed distribution and angular scattering

Figures 3(a), 3(b), and 3(c) show the isotropic and anisotropic components of the TOF profiles for the HCl($v=1$, $J=1,3,5$) products, obtained on the $R(1)$, $R(3)$, and $R(5)$ lines of the $F\,^1\Delta_2-X\,^1\Sigma(1,1)$ band. The profiles are fit to a linear combination of basis functions using a maximum-

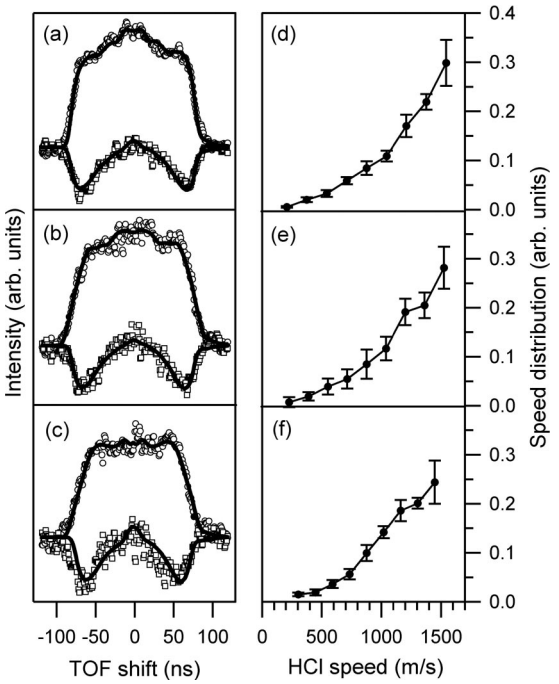

FIG. 3. Isotropic $I_{iso}=I_{\parallel}+2I_{\perp}$ and anisotropic $I_{aniso}=2(I_{\parallel}-I_{\perp})$ components of the core-extracted TOF profiles of the (a) HCl($v=1$, $J=1$), (b) HCl($v=1$, $J=3$), and (c) HCl($v=1$, $J=5$) products from the reaction of atomic chlorine with methanol. The open circles are the measured isotropic TOF profiles, the open squares are the measured anisotropic TOF profiles, and the solid lines are the results of the fit. The speed distributions of the (d) HCl($v=1$, $J=1$), (e) HCl($v=1$, $J=3$), and (f) HCl($v=1$, $J=5$), products are obtained from the isotropic TOF profile. The error bars represent 95% confidence intervals of replicate measurements.

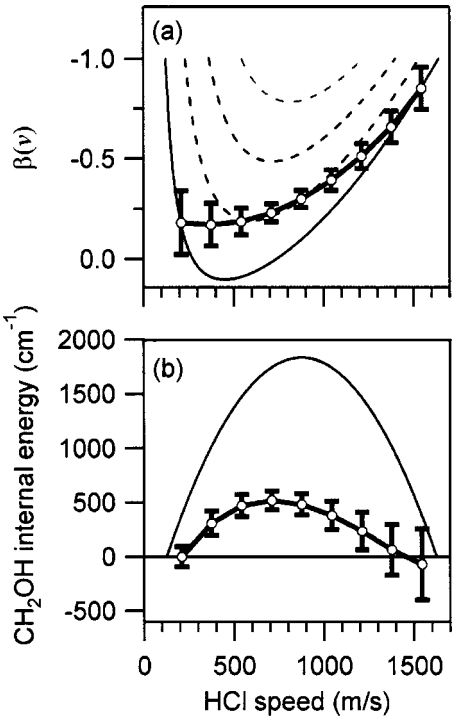

FIG. 4. (a) Speed-dependent spatial anisotropy of the HCl($v=1$, $J=1$) product obtained by fitting the core-extracted anisotropic TOF profiles. The error bars represent 95% confidence intervals of replicate measurements. The outermost curve (thin, solid line) shows the predicted form for $\beta_{HCl}(v_{HCl})$ assuming no CH_2OH internal excitation; the inner curves (thin, dotted lines) are spaced by 500 cm^{-1} in hydroxymethyl radical excitation. (b) CH_2OH internal excitation plotted as a function of HCl speed. This plot results from a transformation of the data shown in (a), as detailed in the text. The thin solid line represents the maximum allowed internal excitation of the CH_2OH products.

entropy analysis.[49] The resulting speed distributions, illustrated in Figs. 3(d), 3(e), and 3(f), show a steady increase of products from the slowest to the fastest speeds. Although the HCl($v=1$) products take up most of the reaction energy, over 1500 cm^{-1} of available energy is still available to populate the internal modes of CH_2OH. Consequently, knowledge of the internal energy of the CH_2OH co-product is necessary to determine accurately $\vec{u}_{HCl}$, which is required to transform the speed distribution into a DCS. This information is obtained from the anisotropic component of the TOF. Figure 4(a) shows the resulting speed-dependent spatial anisotropy, $\beta_{HCl}(v_{HCl})$, of the HCl($v=1$, $J=1$) product along with several calculated curves that are spaced by 500 cm^{-1} in hydroxymethyl radical internal excitation. From this graph, it is clear that the product spatial anisotropy follows the outermost curves, indicating that little internal energy is deposited into the CH_2OH co-product. The measured speed-dependent spatial anisotropy can be converted into the speed-dependent average internal energy of the CH_2OH co-product by noting that

$$\beta_{HCl}(v_{HCl})=\beta_{Cl}P_2(\cos\alpha), \tag{1}$$

where $P_2(x)$ is the second Legendre polynomial, and rearranging the formulas of Shafer *et al.*,[63]

$$E^{int}_{CH_2OH}(v_{HCl})=E_{col}-\Delta E-E^{int}_{HCl} - \frac{m_{HCl}(m_{HCl}+m_{CH_2OH})}{2m_{CH_2OH}}\left(v^2_{HCl}+u^2_{com} - 2v_{HCl}u_{com}\sqrt{\frac{-2\beta(v_{HCl})+1}{3}}\right). \tag{2}$$

Here, E_{col} is the collision energy, ΔE is the difference in potential energy of the reactants and products, E^{int}_{HCl} is the energy of the detected product state, and m_{CH_2OH} and m_{HCl} are the masses of CH_2OH and HCl, respectively. The result of this transformation of coordinates is shown in Fig. 4(b) along with an inverted parabola representing the maximum internal energy allowed for the CH_2OH product. From this graph, it is evident that the internal energy of the CH_2OH product is maximal at the slowest speeds and approaches zero at the fastest speeds. Weighting the experimental curve by the measured speed distribution gives $\langle E^{int}_{CH_2OH}\rangle=170\pm210\,cm^{-1}$. Although the anisotropy gives an average measure of the internal energy of the CH_2OH product, it does not provide information about the distribution of internal states. Assuming that the distribution is peaked about the average, however, the measured speed distribution of the HCl($v=1$, $J=1$) can be converted to a DCS as shown in Fig. 5(a). The vertical error bars again represent 95% confidence inter-

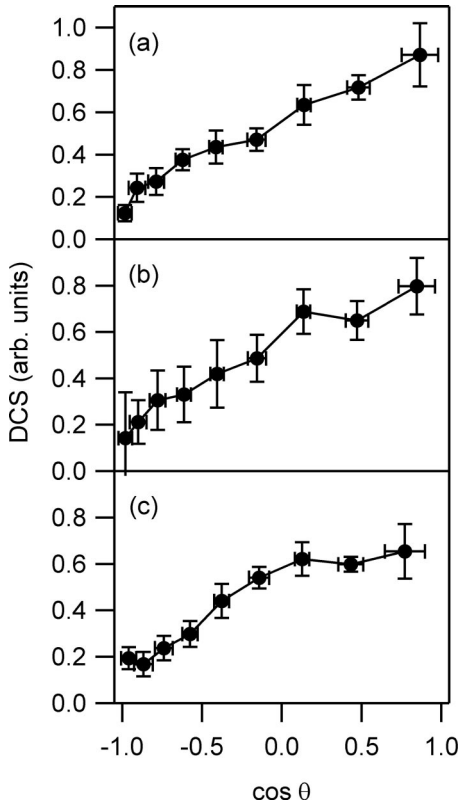

FIG. 5. Differential cross sections for the (a) HCl($v=1$, $J=1$), (b) HCl($v=1$, $J=3$), and (c) HCl($v=1$, $J=5$) products, calculated from the measured speed distribution shown in Fig. 3. The average energy calculated from the speed-dependent spatial anisotropy in Fig. 4 were used to convert the measured HCl speed distribution into a DCS. The vertical error bars represent 95% confidence intervals of replicate measurements. The horizontal error bars result from the error in the measurement of $E^{\text{int}}_{\text{CH}_2\text{OH}}(v_{\text{HCl}})$.

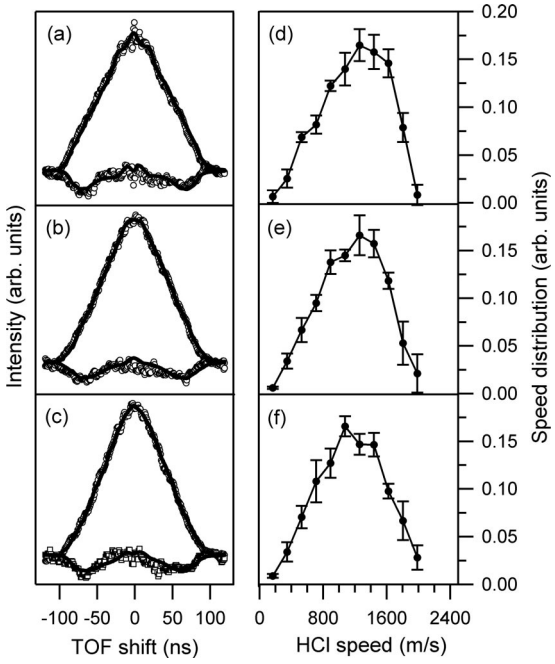

FIG. 6. Isotropic $I_{\text{iso}}=I_{\parallel}+2I_{\perp}$ and anisotropic $I_{\text{aniso}}=2(I_{\parallel}-I_{\perp})$ components of the core-extracted TOF profiles of the (a) HCl($v=0$, $J=3$), (b) HCl($v=0$, $J=5$), and (c) HCl($v=0$, $J=7$) products from the reaction of atomic chlorine with methanol. The open circles are the measured isotropic TOF profiles, the open squares are the measured anisotropic TOF profiles, and the solid lines are the results of the fit. The speed distributions of the (d) HCl($v=0$, $J=3$), (e) HCl($v=0$, $J=5$), (f) HCl($v=0$, $J=7$), products are obtained from the isotropic TOF profile. The error bars represent 95% confidence intervals of replicate measurements.

vals of replicate measurements, and the horizontal error bars represent the error in determining the CH_2OH co-product internal energy from the spatial anisotropy. Figure 5 also shows the DCSs of the HCl($v=1$, $J=3$) and HCl($v=1$, $J=5$) products, which were obtained by performing a similar analysis. Based on this information, it is clear that (1) the measured HCl($v=1$) products are predominantly forward scattered, and (2) the scattering distribution appears to be independent of rotational state.

C. HCl($v=0$) speed distribution and energy disposal

Figures 6(a), 6(b), and 6(c) show the isotropic and anisotropic components of the HCl($v=0$, $J=3,5,7$) TOFs obtained on the $R(3)$, $R(5)$, and $R(7)$ lines of the $F\,^1\Delta_2-X\,^1\Sigma(1,1)$ band. The TOF profiles and consequently the speed distributions [Figs. 6(d), 6(e), and 6(f)] of these product states are nearly indistinguishable. Figure 7(a) shows the measured spatial anisotropy of the HCl($v=0$, $J=5$) product along with several calculated curves spaced by 1000 cm^{-1} in CH_2OH internal excitation. The experimental curve does not follow the ground state curve (thin, black line) and instead more closely follows the curves that correspond to 2000 and 3000 cm^{-1} of CH_2OH internal energy. Application of Eq. (2) to the measured spatial anisotropy gives $E^{\text{int}}_{\text{CH}_2\text{OH}}(v_{\text{HCl}})$, as shown in Fig. 7(b), and $\langle E^{\text{int}}_{\text{CH}_2\text{OH}}\rangle=2210\pm260\,\text{cm}^{-1}$, which is almost 50% of the available energy. For the HCl($v=0$, J) products coincident with CH_2OH having little internal energy, the kinematics are such that $\vec{u}_{\text{HCl}}$ is greater than $\vec{u}_{\text{com}}$. As a consequence, the angle $\boldsymbol{\alpha}$ can be greater than 90° for the speeds at $v=165$, 350, and 530 m/s, eliminating the one-to-one correspondence between the measured spatial anisotropy and CH_2OH internal energy. Here, we have assumed that the internal energy of the CH_2OH co-product does not have a discontinuity as a function of HCl speed. Because there is little population in the speed distribution for these speeds, this assumption has little effect on the calculation of the average internal energy of the CH_2OH co-products. The average energy of the CH_2OH products produced in coincidence with the HCl($v=0$, $J=3$) and HCl($v=0$, $J=7$) products is determined by a similar analysis and found to be nearly identical. The amount of internal energy present in the CH_2OH products is consistent with the imaging experiments of Ahmed *et al.*[38,39] as well as with recent measurements by Kitsopoulos and co-workers.[65] This agreement lends additional support to our findings.

As stated above, there is a possibility that the HCl($v=0$, $J=5$) products are formed with a distribution of CH_2OH internal states. Under the present experimental conditions, the different contributions of these CH_2OH states to the speed distribution cannot be separated to determine a state-specific value for the magnitude of $\vec{u}_{\text{HCl}}$. Consequently, the transformation of the speed distribution to a DCS cannot be performed with any reasonable confidence level.

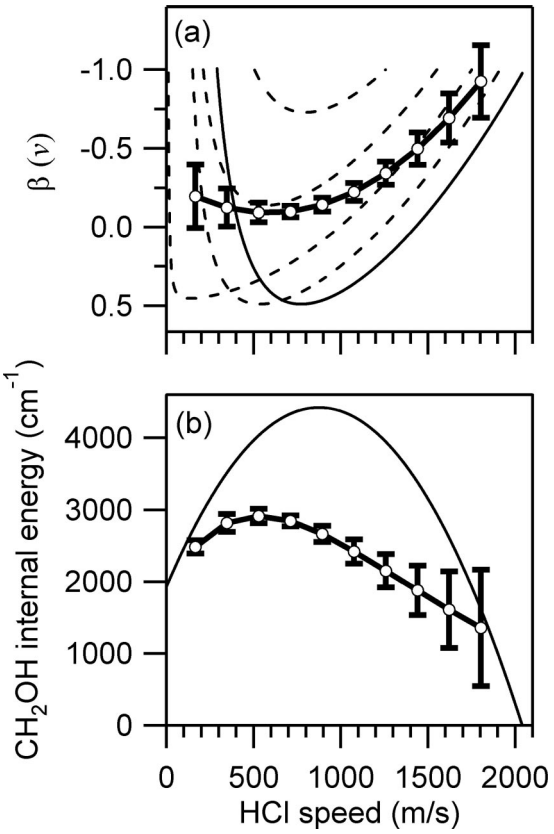

FIG. 7. (a) Speed-dependent spatial anisotropy of the HCl($v=0$, $J=5$) product obtained by fitting the core-extracted anisotropic TOF profiles. The error bars represent 95% confidence intervals of replicate measurements. The outermost curve (thin, solid line) shows the predicted form for $\beta_{\mathrm{HCl}}(v_{\mathrm{HCl}})$ assuming no CH_2OH internal excitation; the inner curves (thin, dotted lines) are spaced by 1000 cm^{-1} in hydroxymethyl radical excitation. (b) CH_2OH internal excitation plotted as a function of HCl speed. This plot results from a transformation of the data shown in (a), as detailed in the text. The thin solid line represents the maximal internal excitation of the CH_2OH products.

IV. DISCUSSION

A. Product branching

One of the most remarkable features of the $Cl+CH_3OH$ reaction is that the HCl products are formed exclusively with the hydroxymethyl radical CH_2OH and not with the methoxy radical CH_3O, despite both channels being energetically allowed under our experimental conditions. The presence of three equivalent hydrogen atoms on the methyl group as opposed to the one hydroxyl hydrogen atom does not account for this selectivity. Although the predominance of the CH_2OH channel may be expected based on the different reaction enthalpies (the CH_2OH channel is exothermic and the CH_3O channel is slightly endothermic), Donahue and co-workers[66–70] caution that reaction enthalpy, by itself, cannot explain radical reactivity for H-atom transfer. Instead, they propose that the barrier to a gas-phase radical-molecule reaction is controlled by an avoided curve crossing of ground and ionic states of the reactants and products. The polar O–H bond is anticipated to have a larger electronic rearrangement than the nonpolar C–H bond in going from reactants to products, and as a consequence, the CH_3O channel should have a larger barrier.[71] Indeed, *ab initio* calculations have indicated that the barrier for the CH_3O channel is as high as 2700–4000 cm^{-1}, whereas the barrier for the CH_2OH channel is nearly nonexistent.[47] This argument, alone, could account for the observed product branching ratio.

Still another mechanism should be considered. It is possible that the dipole moment of the O–H moiety orients the incoming Cl atom so that the electrons in one of its lone pairs form a hydrogen bond with the CH_3OH reagent, similar to the reactions of OH with carboxylic acids and ketones.[72] The unpaired electron in the *p*-orbital on Cl will point perpendicular to the short-lived CH_3O–H–Cl complex, causing the Cl atom to react exclusively with a hydrogen atom on the methyl group.[73] The effect of this dipole interaction between the Cl atom and OH group might be diminished because *ab initio* calculations[47] suggest that the favored prereaction complex ties up the unpaired electron of the Cl atom with the O atom in a two-center, three-electron bond. As our measurements of the CH_2OH channel are most consistent with direct mechanisms, as discussed below, we believe that any dipole interaction between the Cl atom and OH group is simply a steering effect, rather than causing a stable intermediate complex. Both proposed mechanisms may account for the selectivity in the $Cl+CH_3OH$ reaction, but there may be more complexity than these simple models indicate. Vibrational excitation of the O–H bond might distinguish between the contributions of these two possible mechanisms. It should provide further insights into the cause of the CH_2OH selectivity because motion along this coordinate should substantially reduce the barrier to the CH_3O channel.

TABLE I. Energy disposal in the $Cl+CH_3OH \rightarrow HCl+CH_2OH$ reaction. The fractional HCl vibrational populations $f_{\mathrm{vib}}(\mathrm{HCl})$ are normalized such that the sum over all HCl products is equal to 1, i.e., $\Sigma\, P(v,J)=1$.

Product state	$f_{\mathrm{vib}}(\mathrm{HCl})$	$\langle E_{\mathrm{rot}}\rangle$ (cm^{-1})	$\langle E^{\mathrm{int}}_{CH_2OH}\rangle$ (cm^{-1})
HCl($v=0$, J)	0.84±0.07	390±70	
$J=3$			2320±310
$J=5$			2210±260
$J=7$			1960±300
HCl($v=1$, J)	0.16±0.07	190±30	
$J=1$			170±210
$J=3$			160±240
$J=5$			220±260

B. Energy disposal

Table I summarizes the energy disposal for the CH_2OH channel of the $Cl+CH_3OH$ reaction. As dictated by conservation of energy, the internal energy deposited into HCl and CH_2OH products is anticorrelated: when HCl($v=0$) is formed, it is rotationally excited and the CH_2OH co-product possesses large amounts of internal energy; when HCl($v=1$) is formed, it is rotationally cooler and the CH_2OH co-product has significantly less internal energy. These results suggest that at least two mechanisms are present in the $Cl+CH_3OH$ reaction. The large degree of excitation in the CH_2OH products coincident with the HCl($v=0$, J) products indicates that CH_2OH is an active participant, not a spectator, in this channel of the $Cl+CH_3OH$ reaction. In contrast,

the low degree of excitation in the CH_2OH radical coincident with $HCl(v=1, J)$ products is more reminiscent of the spectator model.

C. Formation of HCl($v=1$): Stripping mechanism

Additional evidence for the spectator model can be found by comparing the $HCl(v=1)$ angular distributions of the $Cl+CH_3OH$ reaction to the $HCl(v=1)$ angular distributions of the $Cl+CH_4(v_3=1)$ reaction. For low rotational states, the two reactions have similar forward-scattered DCSs. As the rotational quantum number increases, however, the DCSs of the $HCl(v=1)$ products from the $Cl+CH_4(v_3=1)$ reaction become more back-scattered, in contrast to the DCSs of the $HCl(v=1)$ products from the $Cl+CH_3OH$ reaction. Simpson *et al.*[12] attributed the scattering behavior in the $Cl+CH_4(v_3=1)$ reaction to a competition between two different reaction mechanisms: a *stripping* mechanism and a *rebound* mechanism. The stripping mechanism, resulting from collisions at high impact parameter, gives forward-scattered HCl products, whereas the rebound mechanism, resulting from collisions at low impact parameter, gives back-scattered products. The lack of a sharp, back-scattered component in the $HCl(v=1)$ DCSs of the $Cl+CH_3OH$ reaction, even at high rotational levels, indicates that the rebound mechanism is not a major contributor to the $HCl(v=1)$ products; instead, based on the observed forward-scattered behavior, we believe that these products arise primarily from a stripping mechanism. Because this mechanism does not involve an impulsive release of energy, the rotational modes of either product should be relatively unexcited, as observed.

The stripping mechanism also explains an apparent failure of the kinematic model proposed by Picconatto *et al.*[74] According to their model, the internal energy is constrained by kinematic factors that involve ''reflection'' off the repulsive wall of the potential energy surface. For $H+LH \rightarrow HL+H$ systems, where a heavy atom abstracts a light atom, most of the energy available for products comes from the exothermicity of the reagents because the translational energy is severely restricted. This constraint reduces the available energy for the products of the $Cl+CH_3OH$ reaction from 4740 cm^{-1} to 2900 cm^{-1}. Although the maximum observable $HCl(v=0)$ J state is well below this energetic limit ($J_{max}=16$), most of the $HCl(v=1)$ products are not energetically allowed according to the kinematic constraint and are consequently in apparent violation of the model. The kinematic limit, however, is derived from the assumption of a collinear approach of the Cl atom towards the C–H bond. If the trajectory of the Cl atom has a perpendicular approach, as is the case for the stripping mechanism, the trajectory samples a different portion of the potential energy surface and the reflection off the inner corner of the potential energy surface is less constrained. Thus, more translational energy is available to populate the internal modes of the products. The failure of the kinematic model for noncollinear transition state geometries has been observed previously in other reactions[12,75] and will be the topic of a forthcoming paper.[76]

It is interesting to note that our $HCl(v=1)$ rotational distribution of the $Cl+CH_3OH$ reaction is similar to the $HCl(v=1)$ rotational distribution of the $Cl+CH_3CH_2OH$ reaction, as measured by Rudić *et al.*[41] Although rotational distributions alone are not sufficient to elucidate the detailed mechanism of a reaction, the similarities between the two distributions may indicate that the stripping mechanism is also responsible for the formation of the vibrationally excited HCl products in the $Cl+CH_3CH_2OH$ reaction. The stripping mechanism has been found to play a significant role in hydrogen-atom abstraction reactions involving other vibrationally cold hydrocarbons as well.[18,19] In the Cl+propane reaction, Blank *et al.*[18] determined that collisions with large impact parameters preferentially abstracted a secondary hydrogen atom via the stripping mechanism, resulting in forward-scattered products. As in the case with the $Cl+CH_4(v_3=1)$ reaction, collisions at larger impact parameters are possible because the barrier is greatly diminished or negligible.

D. Formation of HCl($v=0$): Impulse release mechanism

Blank *et al.*[18] also found that collisions at smaller impact parameters involved a direct mechanism with an impulsive product recoil that left significant energy in the internal modes of the C_3H_7 products. The previous studies of Ahmed *et al.*[38,39] on the $Cl+CH_3OH$ reaction suggest that such a rebound mechanism may be responsible for the $HCl(v=0)$ products we observe. Using single-photon ionization at 157 nm, they detected all the CH_2OH products without state selection and found them to be mostly forward-scattered with respect to the Cl beam. Given that the $HCl(v=1)$ products are predominantly forward-scattered, the $HCl(v=0)$ DCSs must have a significant back-scattered component in order to match the scattering distribution of the measured CH_2OH products. Indeed, recent experiments by Kitsopoulos and co-workers[65] suggest that the $HCl(v=0,J)$ DCSs are sharply peaked in the backward direction. A simple line-of-centers analysis would indicate that the back-scattered $HCl(v=0)$ products are preferentially formed at small impact parameters, which is characteristic of a rebound mechanism. The measurements of Kitsopoulos and co-workers,[65] however, also show that there is a significant forward-scattered component in the DCSs of the $HCl(v=0)$ products formed in low rotational states, suggesting that a stripping mechanism plays a role in the formation of the $HCl(v=0)$ products as well. Although our measurements do not indicate a change in reactive mechanism as a function of rotational state, the speed-dependent spatial anisotropy shows that less energy is deposited into the CH_2OH internal degrees of freedom at higher speeds, which is consistent with the possibility of a stripping mechanism in the forward-scattered direction. The presence of both rebound and stripping mechanisms indicates that the $HCl(v=0)$ states are formed from collisions at a wide range of impact parameters.

A rebound mechanism is generally associated with an impulsive release of energy in order to redirect the Cl-atom momentum. This impulsive release would create a large torque on the hydroxymethyl radical because the C–H bond

does not pass through the CH_2OH center of mass. As a consequence, the CH_2OH products would be rotationally excited, providing a source of the extensive internal energy we observe in the CH_2OH product. The other source of internal energy in the CH_2OH product may be the wagging vibration of the hydrogen atoms in the CH_2 group, arising from the relaxation of the bent CH_2 group in the transition state to the planar geometry in the free hydroxymethyl radical. If vibrational excitation of the CH_2 wagging mode ($v_9 = 234\,\mathrm{cm}^{-1}$) (Ref. 42) were the sole source of internal energy of the CH_2OH radical, close to 10 quanta of excitation would be necessary to account for the measured internal energy. This high degree of excitation is improbable, and consequently, the internal energy most likely arises from a combination of vibrational and rotational modes. The trajectories of Rudić *et al.*[48] in fact indicate that most of the internal energy is accounted for by rotational energy.

The $Cl+C_2H_6$ reaction is an obvious reference to our current measurements because ethane and methanol have similar structures and the predominant abstraction channel in the $Cl+CH_3OH$ reaction is from the hydrogen located on the methyl group, not the hydroxyl group. Furthermore, the $Cl+C_2H_6$ reaction has been examined previously under similar conditions and collision energies ($1900\pm210\ \mathrm{cm}^{-1}$). Kandel *et al.*[14] found the $HCl(v=0)$ rotational distribution to be cold, $\langle E_{\mathrm{rot}}\rangle = 48\pm3\ \mathrm{cm}^{-1}$, and the scattering distributions to be nearly isotropic. These seemingly contradictory features indicate that the $Cl+C_2H_6$ reaction proceeds through a loosely constrained transition-state geometry that does not have a sudden, impulsive H-atom transfer. The $HCl(v=0)$ rotational distribution from the $Cl+CH_3OH$ reaction, on the other hand, is much warmer, $\langle E_{\mathrm{rot}}\rangle = 390\pm70\ \mathrm{cm}^{-1}$ and accounts for ~13% of the available energy according to the kinematic model. Although the conversion of the total $Cl+CH_3OH$ reaction energy into rotational energy is by no means efficient, it is more than twice as efficient than in the $Cl+C_2H_6$ reaction, where a mere 5% of the available energy[14] is converted into rotation according to the kinematic model. The additional degree of $HCl(v=0)$ rotational excitation in the $Cl+CH_3OH$ reaction may indicate a larger impulse release along the breaking C–H bond, which supports the rebound mechanism proposed above. A larger impulsive release in the $Cl+CH_3OH$ reaction might be expected because of the greater exothermicity (~2780 cm^{-1}) as compared to the $Cl+C_2H_6$ reaction (~930 cm^{-1}).

Rudić *et al.*,[40,41] however, has proposed an alternative explanation for the warmer HCl rotational distribution of the $Cl+CH_3OH$ reaction: the rotation of the HCl products are accelerated by the dipole–dipole interaction between the HCl and the O atom on the CH_2OH radical before these two products separate. Their conclusions were based on classical trajectories performed on *ab initio* potential energy surfaces and measured rotational distributions of several oxygen-containing organic molecules, including methanol, ethanol, and dimethyl ether. The trajectories show no evidence of complex formation, but the proximity of the oxygen atom appears to influence the dynamics of the abstracted hydrogen atom, causing increased rotation in both products. Our current measurements cannot differentiate between the two mechanisms, impulsive release or dipole–dipole interaction, because both cause significant rotation of the product states. These mechanisms are not mutually exclusive, however, and it is possible that both contribute to the overall dynamics of the $Cl+CH_3OH$ reaction.

E. Concluding remarks

A combination of molecular beam and laser techniques has allowed us to investigate the $Cl+CH_3OH$ reaction in exquisite detail. This polyatomic system displays a rich dynamical behavior in which different HCl vibrational states are associated with different reaction mechanisms. It is hoped that these experimental findings will stimulate theoretical investigations into this reaction system, although it must be appreciated at once that the size of the system makes such computations quite labor intensive.

ACKNOWLEDGMENTS

Two of the authors (H.A.B. and J.P.C.) thank the National Science Foundation for graduate fellowships. H.A.B. also acknowledges Stanford University for the award of a Stanford Graduate Fellowship. The authors thank Davida J. Ankeny Brown for a careful reading of the paper and Andrew Orr-Ewing for providing us with unpublished manuscripts. This material is based upon work supported by the National Science Foundation under Grant No. 0242103.

[1] D. J. Bogan and D. W. Setser, J. Chem. Phys. **64**, 586 (1976).
[2] M. A. Nazar and J. C. Polanyi, Chem. Phys. **94**, 299 (1981).
[3] M. A. Wickramaaratchi, D. W. Setser, H. Hildebrandt, B. Korbitzer, and H. Heydtmann, Chem. Phys. **94**, 109 (1985).
[4] K. I. Sugawara, F. Ito, T. Nakanaga, H. Takeo, and C. Matsumura, J. Chem. Phys. **92**, 5328 (1990).
[5] W. W. Harper, S. A. Nizkorodov, and D. J. Nesbitt, J. Chem. Phys. **113**, 3670 (2000).
[6] W. W. Harper, S. A. Nizkorodov, and D. J. Nesbitt, Chem. Phys. Lett. **335**, 381 (2001).
[7] J. J. Lin, J. Zhou, W. Shiu, and K. Liu, Science **300**, 966 (2003).
[8] J. Zhou, J. J. Lin, W. Shiu, and K. Liu, J. Chem. Phys. **119**, 2538 (2003).
[9] J. Zhou, J. J. Lin, W. Shiu, and K. Liu, J. Chem. Phys. **119**, 4997 (2003).
[10] J. Zhou, J. J. Lin, and K. Liu, J. Chem. Phys. **119**, 8289 (2003).
[11] J. H. Park, Y. S. Lee, J. F. Hershberger, J. M. Hossenlopp, and G. W. Flynn, J. Am. Chem. Soc. **114**, 58 (1992).
[12] W. R. Simpson, T. P. Rakitzis, S. A. Kandel, A. J. Orr-Ewing, and R. N. Zare, J. Chem. Phys. **103**, 7313 (1995).
[13] W. R. Simpson, T. P. Rakitzis, S. A. Kandel, T. Levon, and R. N. Zare, J. Phys. Chem. **100**, 7938 (1996).
[14] S. A. Kandel, T. P. Rakitzis, T. Levon, and R. N. Zare, J. Chem. Phys. **105**, 7550 (1996).
[15] D. F. Varley and P. J. Dagdigian, J. Phys. Chem. **99**, 9843 (1995).
[16] D. F. Varley and P. J. Dagdigian, J. Phys. Chem. **100**, 4365 (1996).
[17] D. F. Varley and P. J. Dagdigian, Chem. Phys. Lett. **255**, 393 (1996).
[18] D. A. Blank, N. Hemmi, A. G. Suits, and Y. T. Lee, Chem. Phys. **231**, 261 (1998).
[19] N. Hemmi and A. G. Suits, J. Chem. Phys. **109**, 5338 (1998).
[20] A. C. Luntz and P. Andresen, J. Chem. Phys. **72**, 5851 (1980).
[21] A. C. Luntz, J. Chem. Phys. **73**, 1143 (1980).
[22] P. Andresen and A. C. Luntz, J. Chem. Phys. **72**, 5842 (1980).
[23] K. Kleinermanns and A. C. Luntz, J. Chem. Phys. **77**, 3533 (1982).
[24] K. Kleinermanns and A. C. Luntz, J. Chem. Phys. **77**, 3537 (1982).
[25] K. Kleinermanns and A. C. Luntz, J. Chem. Phys. **77**, 3774 (1982).
[26] X. Liu, R. L. Gross, G. E. Hall, J. T. Muckerman, and A. Suits, J. Chem. Phys. **117**, 7947 (2002).
[27] F. Ausfelder and K. G. McKendrick, Prog. React. Kinet. **25**, 299 (2000).
[28] F. Ausfelder, H. Kelso, and K. G. McKendrick, Phys. Chem. Chem. Phys. **4**, 473 (2002).

[29] T. Suzuki and E. Hirota, J. Chem. Phys. **98**, 2387 (1993).
[30] M. Brouard, H. M. Lambert, J. Short, and J. P. Simons, J. Phys. Chem. **99**, 13571 (1995).
[31] J. J. Lin, S. Harich, Y. T. Lee, and X. Yang, J. Chem. Phys. **110**, 10821 (1999).
[32] J. J. Lin, Y. T. Lee, and X. Yang, J. Chem. Phys. **109**, 2975 (1998).
[33] J. J. Lin, J. Shu, Y. T. Lee, and X. Yang, J. Chem. Phys. **113**, 5287 (2000).
[34] N. J. Dutton, I. W. Fletcher, and J. C. Whitehead, J. Phys. Chem. **89**, 569 (1985).
[35] B. S. Agrawalla and D. W. Setser, J. Phys. Chem. **90**, 2450 (1986).
[36] S. Bradforth, D. W. Arnold, R. B. Metz, A. Weaver, and D. M. Neumark, J. Phys. Chem. **95**, 8066 (1991).
[37] H. Umemoto, K. Kongo, S. Inaba, Y. Sonoda, T. Takayanagi, and Y. Kurosaki, J. Phys. Chem. A **103**, 7026 (1999).
[38] M. Ahmed, D. S. Peterka, and A. G. Suits, Chem. Phys. Lett. **317**, 264 (2000).
[39] M. Ahmed, D. S. Peterka, and A. G. Suits, Phys. Chem. Chem. Phys. **2**, 861 (2000).
[40] S. Rudić, D. Ascenzi, and A. J. Orr-Ewing, Chem. Phys. Lett. **332**, 487 (2000).
[41] S. Rudić, C. Murray, D. Ascenzi, H. Anderson, J. N. Harvey, and A. J. Orr-Ewing, J. Chem. Phys. **117**, 5692 (2002).
[42] R. D. Johnson III and J. W. Hudgens, J. Phys. Chem. **100**, 19874 (1996).
[43] L. A. Curtiss, K. Raghavachari, P. C. Redfern, and J. A. Pople, J. Chem. Phys. **106**, 1063 (1997).
[44] B. Ruscic and J. Berkowitz, J. Chem. Phys. **95**, 4033 (1991).
[45] G. S. Tyndall, J. J. Orlando, C. S. Kegley-Owen, T. J. Wallington, and M. D. Hurley, Int. J. Chem. Kinet. **31**, 776 (1999).
[46] S. Dobe, T. Berces, F. Temps, H. G. Wagner, and H. Ziemer, *Proceedings of the 25th Symposium (International) on Combustion* (Combustion Institute, Pittsburgh, PA, 1994), pp. 775.
[47] J. T. Jodkowski, M.-T. Rayez, J.-C. Rayez, T. Berces, and S. Dobe, J. Phys. Chem. A **102**, 9230 (1998).
[48] S. Rudić, C. Murray, J. N. Harvey, and A. J. Orr-Ewing, J. Chem. Phys. **120**, 186 (2004).
[49] W. R. Simpson, A. J. Orr-Ewing, T. P. Rakitzis, S. A. Kandel, and R. N. Zare, J. Chem. Phys. **103**, 7299 (1995).
[50] J. P. Camden, H. A. Bechtel, and R. N. Zare, Rev. Sci. Instrum. **75**, 556 (2004).
[51] P. C. Samartzis, B. Bakker, T. P. Rakitzis, D. H. Parker, and T. N. Kitsopoulos, J. Chem. Phys. **110**, 5201 (1999).
[52] W. J. van der Zande, R. Zhang, R. N. Zare, K. G. McKendrick, and J. J. Valentini, J. Phys. Chem. **95**, 8205 (1991).
[53] S. Arepalli, N. Presser, D. Robie, and R. J. Gordon, Chem. Phys. Lett. **118**, 88 (1985).
[54] R. Callaghan, S. Arepalli, and R. J. Gordon, J. Chem. Phys. **86**, 5273 (1987).
[55] Y. Xie, P. T. A. Reilly, S. Chilukuri, and R. J. Gordon, J. Chem. Phys. **95**, 854 (1991).
[56] D. S. Green, G. A. Bickel, and S. C. Wallace, J. Mol. Spectrosc. **150**, 303 (1991).
[57] D. S. Green, G. A. Bickel, and S. C. Wallace, J. Mol. Spectrosc. **150**, 354 (1991).
[58] D. S. Green, G. A. Bickel, and S. C. Wallace, J. Mol. Spectrosc. **150**, 388 (1991).
[59] E. A. Rohlfing, D. W. Chandler, and D. H. Parker, J. Chem. Phys. **87**, 5229 (1987).
[60] A. Yokoyama and T. Takayanagi, Chem. Phys. Lett. **307**, 48 (1999).
[61] P. J. Dagdigian, D. F. Varley, R. Liyanage, R. J. Gordon, and R. W. Field, J. Chem. Phys. **105**, 10251 (1996).
[62] W. C. Wiley and I. H. McLaren, Rev. Sci. Instrum. **26**, 1150 (1955).
[63] N. E. Shafer, A. J. Orr-Ewing, W. R. Simpson, H. Xu, and R. N. Zare, Chem. Phys. Lett. **212**, 155 (1993).
[64] J. D. Smith, J. D. DeSain, and C. A. Taatjes, Chem. Phys. Lett. **366**, 417 (2002).
[65] C. Murray, A. J. Orr-Ewing, R. L. Toomes, and T. N. Kitsopoulos, J. Chem. Phys. **120**, 2230 (2004).
[66] N. M. Donahue, J. S. Clarke, and J. G. Anderson, J. Phys. Chem. A **102**, 3923 (1998).
[67] J. S. Clarke, J. H. Kroll, N. M. Donahue, and J. G. Anderson, J. Phys. Chem. A **102**, 9847 (1998).
[68] J. S. Clarke, N. M. Donahue, J. H. Kroll, H. A. Rypkema, and J. G. Anderson, J. Phys. Chem. **104**, 5254 (2000).
[69] N. M. Donahue, J. Phys. Chem. A **105**, 1489 (2001).
[70] H. A. Rypkema, N. M. Donahue, and J. G. Anderson, J. Phys. Chem. A **105**, 1498 (2001).
[71] H. A. Rypkema (private communication).
[72] I. W. M. Smith and A. R. Ravishankara, J. Phys. Chem. A **106**, 4798 (2002).
[73] B. J. Ellison (private communication).
[74] C. A. Picconatto, A. Srivastava, and J. J. Valentini, J. Chem. Phys. **114**, 1663 (2001).
[75] H. A. Bechtel, J. P. Camden, D. J. A. Brown, and R. N. Zare, J. Chem. Phys. (in press).
[76] A. E. Pomerantz, F. Ausfelder, and R. N. Zare (in preparation).